



**HAL**  
open science

## Determination of methane, ethane and propane on activated carbons by experimental pressure swing adsorption method

Bich Ngoc Ho, David Pino-Perez, Camélia Matei Ghimbeu, Joseph Diaz, Deneb Peredo-Mancilla, Cécile Hort, David Bessieres

### ► To cite this version:

Bich Ngoc Ho, David Pino-Perez, Camélia Matei Ghimbeu, Joseph Diaz, Deneb Peredo-Mancilla, et al.. Determination of methane, ethane and propane on activated carbons by experimental pressure swing adsorption method. *Journal of Natural Gas Science and Engineering*, 2021, 95, pp.104124. 10.1016/j.jngse.2021.104124 . hal-03445248

**HAL Id: hal-03445248**

**<https://hal.science/hal-03445248>**

Submitted on 16 Oct 2023

**HAL** is a multi-disciplinary open access archive for the deposit and dissemination of scientific research documents, whether they are published or not. The documents may come from teaching and research institutions in France or abroad, or from public or private research centers.

L'archive ouverte pluridisciplinaire **HAL**, est destinée au dépôt et à la diffusion de documents scientifiques de niveau recherche, publiés ou non, émanant des établissements d'enseignement et de recherche français ou étrangers, des laboratoires publics ou privés.



Distributed under a Creative Commons Attribution - NonCommercial 4.0 International License

# Determination of methane, ethane and propane on activated carbons by experimental pressure swing adsorption method

Bich Ngoc Ho<sup>a,b,\*</sup>, David Pino Perez<sup>b,\*\*</sup>, Deneb Peredo Mancilla<sup>b</sup>, Joseph Diaz<sup>b</sup>, Cécile Hort<sup>a</sup>, David Bessieres<sup>b</sup> and Camélia Matei Ghimbeu<sup>c,d</sup>

<sup>a</sup>Université de Pau et des Pays de l'Adour, E2S UPPA, LaTEP, Pau, France

<sup>b</sup>Université de Pau et des Pays de l'Adour, E2S UPPA, CNRS, Total, LFCR, Pau, France

<sup>c</sup>Université de Haute-Alsace, CNRS, Institut de Science des Matériaux de Mulhouse (IS2M) UMR 7361, F-68100 Mulhouse, France

<sup>d</sup>Université de Strasbourg, F-67081 Strasbourg, France

## ARTICLE INFO

### Keywords:

Adsorption isotherms

Natural gas

Methane

Ethane

Propane

Activated carbon

## ABSTRACT

This study focuses on isotherms adsorption of natural gas components i.e. methane, ethane, and propane on five commercial activated carbons to determine their different behaviors towards each compound. These five commercial activated carbons have different textures that are supposed to affect their adsorption capacity. The experiments were carried out at 303K within a pressure range of 0-3 MPa using a homemade manometric adsorption device. A comprehensive process was also detailed with a step-by-step calculation. The obtained data were then fitted into the modified Langmuir model in order to justify the mono-layer coverage. Hence, the relationship between the Langmuir adsorption capacities and different textural properties were plotted, and only the specific area showed its direct influence. The outcome also turned out that the most promising activated carbon is the one that possesses not only the highest specific surface area but also has an adequate balance between the microporous and mesoporous volumes.

## 1. Introduction

Climate change is one of the most considerable environmental threats nowadays. Therefore, the reduction of air pollutant emission has attracted a lot of attention as a global challenge. Taking into account that petroleum and coal are naturally unclean, natural gas is thought to be a promising alternative thanks to its availability, adaptability, high energy value, and low carbon dioxide emission upon combustion. In 2019, the world annual natural gas consumption reached 3,929,000 million m<sup>3</sup>, making it become the third largest energy source [1, 2]. Raw natural gas contains prominently up to 70-90% of methane (CH<sub>4</sub>), other alkanes such as ethane (C<sub>2</sub>H<sub>6</sub>, 6.4%) and propane (C<sub>3</sub>H<sub>8</sub>, 5.3%), butane (C<sub>4</sub>H<sub>10</sub>, 1.4%) and other non-hydrocarbons such as carbon dioxide (CO<sub>2</sub>, 5%) [3]. However, the presence of compounds other than methane decreases the combustion heat capacity of the gas and can lead to the damage of the pipelines, they must be eliminated from natural gas before application [4, 5].

Up to date, numerous physical and chemical treatments for natural gas, some regular methods such as membrane separation, water scrubbing, physical and chemical absorption have been applied in both laboratory and industrial scales and they all have proved their pros and cons [6–8]. Water scrubbing is commonly used thanks to its simple operation and high CH<sub>4</sub> purity outcome, but it requires a huge amount of water use. On the other hand, chemical adsorption by using amines can achieve CH<sub>4</sub> of 98% purity but its needs of chemicals and regeneration energy are undesirable. In order to overcome these issues, pressure swing adsorption (PSA) is suggested due to its effectiveness and its capacity of undesired compounds elimination [9]. PSA can be used to enrich the methane concentration to enhance the calorific value and to meet the gas quality requirement. Moreover, PSA is also promising in sustaining gas production and minimizing pollution problems due to gas flaring [10, 11].

Consequently, the exploration of optimum adsorbents for natural gas purification is in high demand. In our days, material screening is carried out not only in adsorption experiments but also in artificial intelligence such as molecular simulations and machine learning in order to accurately predict the structural relationship between adsorption capacity and structural properties of adsorbents [12–14]. Most of adsorbents studied are zeolites [15–17], silica gels [18], metal-organic frameworks (MOFs) [2, 19] and activated carbons [20–24]. Amongst them, activated carbons have

\*Principal corresponding author

\*\*Corresponding author

✉ [bich-ngoc.ho@univ-pau.fr](mailto:bich-ngoc.ho@univ-pau.fr) (B.N. Ho); [david.pino-perez@univ-pau.fr](mailto:david.pino-perez@univ-pau.fr) (D.P. Perez)

shown their advantageous result comparing to other adsorbents because their production cost are less expensive than others while they still have greater adsorption capacity [25]. Activated carbons can be produced by pyrolysis and activation of natural sources such as rice husk [26], tree wood, bamboo, charcoal, or sometimes rare carbonaceous plant-derived as butnea pollen [27] or clays [28]. They also have been used in water and air purification, dentistry, catalytic chemistry for years, which therefore is supposed to give a promising result in gas pressure swing adsorption technology [29].

A lot of experiments were performed on mostly dominant compounds in natural gas, methane, and carbon dioxide combustion in the research on adsorbents for purification of the raw natural gas [30–32]. However, The elimination of ethane and propane, two other compounds in natural gas, is also desirable to increase its heat combustion [33]. Furthermore, the study of gas adsorption on activated carbon for other hydrocarbons thus allows us to comprehend their potential performance for natural gas purification, hence lead to effective solutions on an industrial scale.

Previously published works have only generally shown that the adsorption of gas molecules onto the surface of activated carbon is influenced by numerous factors such as surface chemistry, morphology, and affinity of the adsorbate with the adsorbent [34, 35]. In this context, the objective of this study is to investigate methane, ethane, and propane isothermal adsorption on five commercial activated carbons and to deduce the relationship between the textural properties of adsorbents and their adsorption performance in both low and high working pressures. The main physical properties of these materials, experimental set-up, and the methodology are detailed in Section Materials and methods. In Results and Discussion, an analysis of the results is provided and the relationship between the structural properties of the activated carbons and the adsorption capacity is deduced. Besides, the experimental outcome was fitted to the modified Langmuir model and compared to various reported results in the literature.

## 2. Materials and method

### 2.1. Gas cylinders and activated carbons

Methane, ethane, propane, and helium were purchased from Linde AG (France), with a purity up to 99.999% (purity denoted 5.0) as described in Table 1. They were conducted to the system via a pressure regulator of the same provider. Propane was exceptionally pumped into a smaller gas tank under a counter-current heating for pre-gasification. Additional purification was not required.

**Table 1**  
CAS registry number and purity of the gas cylinders.

Component	CAS Reg. No.	Purity
Helium	7440-59-7	99.999%
Methane	74-82-8	99.995%
Ethane	74-84-0	99.95%
Propane	74-98-6	99.95%

Five Norit commercial activated carbons named RX 1.5, ROx 0.8, CNR-115, CGRAN, and GAC 1240 were purchased from Cabot Corporation (USA). CGRAN and CNR-115 were chemically activated by  $H_3PO_4$  while RX 1.5, ROx 0.8, and GAC 1240 were activated by steam. The morphology of each activated carbon surface was analyzed by scanning electron microscopy (SEM) using an FEI model Quanta 400 analyzer.

Since the activated carbons were provided commercially, they are considered stable i.e do not lose adsorption capacity over numerous adsorption-desorption cycles. On the industrial scale, depending on the frequency of use, the service time of Norit activated carbons can last for months. Moreover, exhausted commercial activated carbons are able to be thermally or chemically reactivated and returned to 97% or greater compared to virgin carbon with reduced cost [36, 37]. On the laboratory scale, the durability of Norit activated carbons was reported to be constant in Plaza et al. and Aumeier et al., where 5-10 cycles of adsorption-desorption cycles were carried out for different configurations of adsorption [38, 39]. The adsorption capacities of methane, ethane, and propane onto the five activated carbon in this study are hence judged to remain steady.

## 2.2. Experimental system and measurement protocol

### 2.2.1. System set-up

Figure 1 represents A schematic plan of the homemade adsorption system. This system is composed of a dosing cell and an adsorption cell manufactured by Top Industries. Both of them are made from stainless steel and have similar volume ( $18.5 \pm 0.2 \text{ cm}^3$ ). These two cells were put in series and coupled with a PR 400B-S manometer of MKS Instruments, Inc. This manometer is operating in a wide range of pressure 0-3.3 MPa with an accuracy of 0.25% of reading. A heating wire and isolation foam wrap around the whole system to ensure the homogeneity of temperature. The system is also integrated with a temperature sensor and display devices for isotherm monitoring.

### 2.2.2. Sample preparation

An amount of activated carbon ( $0.9 \pm 0.02 \text{ g}$ ) was introduced directly into the cleaned adsorption cell and put under vacuum using a vacuum pump at  $90^\circ\text{C}$  for at least 8 hours. This treatment at high temperature is required for activated carbons to ensure that all water and residual adsorbate molecules are removed from the pores thus guarantee the reliability of the adsorption isotherms.

Once the adsorption was finished, the desorption step was conducted under vacuum at  $90^\circ\text{C}$  for 8 hours again in order to regenerate the performance of the adsorbent.

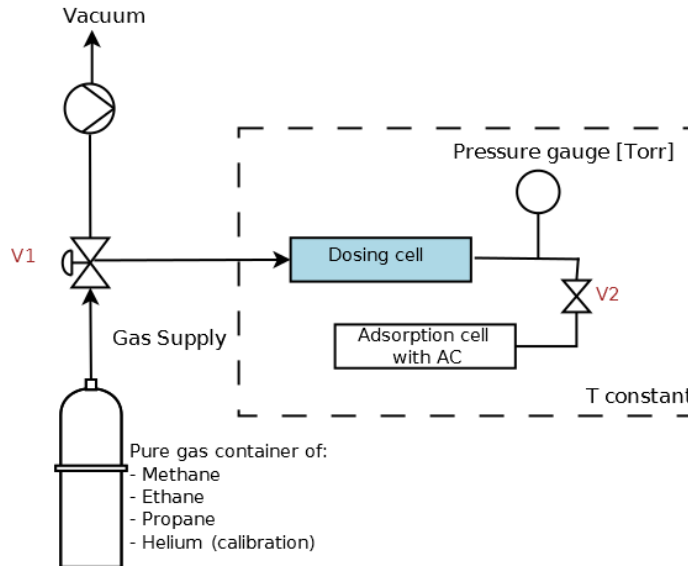


Figure 1: Scheme of pure natural gas adsorption system.

## 2.3. Measurement principle

### 2.3.1. Calibration

Based on the fact that activated carbons do not adsorb noble gas, a helium expansion was undertaken from the dosing cell into the adsorption cell before each measurement to determine the adsorption volume of the system possessing an activated carbon. Knowing the dosage volume  $V_{dos}$  in advance by carbon dioxide calibration, by this consecutive measurement, the calculated adsorption volume is usually inferior to the one without sample.

$$V_{ads} = V_{dos} \left( \frac{P_{dos}}{P_{expa}} \right) \quad (1)$$

where  $P_{dos}$  is the measured pressure of the dosing cell when V2 is closed and  $P_{expa}$  is the total pressure in the whole equipment when V2 is opened. The total volume of the system, denoted  $V_{tot}$  is hence calculated:

$$V_{tot} = V_{dos} + V_{ads} \quad (2)$$

### 2.3.2. Adsorption isotherms

A dose of gas is released into the dosing cell (V1 opened, V2 closed). Once the equilibrium in the dosing cell is stabilized ( $P_{int}$ ), the gas is then released to the adsorption cell by opening V2.

For the first point of the isotherm ( $i = 1$ ), the number of moles of the adsorbate gas introduced in the dosing cell  $n_{tot}^1$  is calculated as in Equation 3:

$$n_{tot}^1 = V_{dos} \cdot \rho_{int}^1 \quad (3)$$

where  $\rho_{int}^1$ , which is also denoted  $\rho_{int}^1(P, T)$  is the molar density of the adsorbate at a particular initial pressure  $P_{int}$  and constant working temperature.  $\rho(P, T)$  is calculated by using Equation 4, which is considered as a polynomial function of  $P$  at 303K and its parameters were obtained from NIST database [40]. The coefficients of different pure gases are showed in Table 2.

$$\rho(P, T) = a \cdot P^4 + b \cdot P^3 + c \cdot P^2 + d \cdot P + e \quad (4)$$

The adsorption isotherms are described through an accumulative process. The adsorption equilibrium is reached when the pressure is stabilized again ( $P_{fin}$ ), the molar quantity of gas adsorbed onto the surface of the adsorbent  $n_{ads}^1$  is calculated as in Equation 5:

$$n_{ads}^1 = n_{tot}^1 - V_{tot} \cdot \rho_{fin}^1 \quad (5)$$

The procedure is repeated by closing V2 and introducing a new dose of gas into the dosing cell.  $n_{tot}$  and  $n_{ads}$  at the  $i$ -th point are calculated as follows [41, 42]:

$$n_{tot}^i = V_{ads} \cdot \rho_{fin}^{i-1} + V_{dos} \cdot \rho_{int}^i \quad (6)$$

**Table 2**

Natural gas compounds kinetic diameters and polynomial parameters [43–45].

Parameter	Methane	Ethane	Propane
Kinetic diameter (pm)	380	400	430
a ( $\cdot 10^{-10}$ )	2.10	2000	2158
b ( $\cdot 10^{-8}$ )	4.35	400	186
c ( $\cdot 10^{-4}$ )	649	4.00	6.66
d	0.04	0.04	0.04
e ( $\cdot 10^{-4}$ )	0	3.00	0
$R^2$	0.99	1	0.99

### 2.3.3. Adsorption isotherms fitting parameters

The Langmuir model is the most popular model used to represent experimental isotherms by assuming that the adsorbate behaves as an ideal gas in isothermal conditions and the adsorbent has an ideal chemically homogeneous solid surface [46, 47]. In this context, the modified Langmuir model was chosen, where we assumed that during the adsorption procedure, the attachment gas molecules onto the surface of activated carbons in the form of a single-layer coverage. We denoted  $n_{ads}^{excess}$  the excess adsorbed quantity of gas at the working pressure called P. The experimental results were then compared to the calculated estimation by using the modified Langmuir model with two parameters [48]:

$$n_{ads}^{excess} = n_L \times \frac{p}{p + p_L} \left( 1 - \frac{\rho_m(p, T)}{\rho_{ads}} \right) \quad (7)$$

where  $p_L$ , called the Langmuir pressure, is the pressure where the adsorbate occupied half of the sites the surface of the activated carbon and  $n_L$  is the maximum amount absorbed, corresponding to the occupancy of all sites. In this

study, the value of  $\rho_{ads}$  had been fixed at  $423 \text{ kg m}^{-3}$  for methane,  $546 \text{ kg m}^{-3}$  for ethane and  $581 \text{ kg m}^{-3}$  for propane [49–51].

Since the Langmuir fitting parameters are determined considering the confirmation of fitted Langmuir equation in low working pressure and its acceptance in high-pressure zone, a deviation standard was thus required and calculated as Equation 8:

$$\Delta n = \frac{1}{N} \sqrt{\sum_{i=1}^N (n_{excess(i)} - n_{FIT})^2} \quad (8)$$

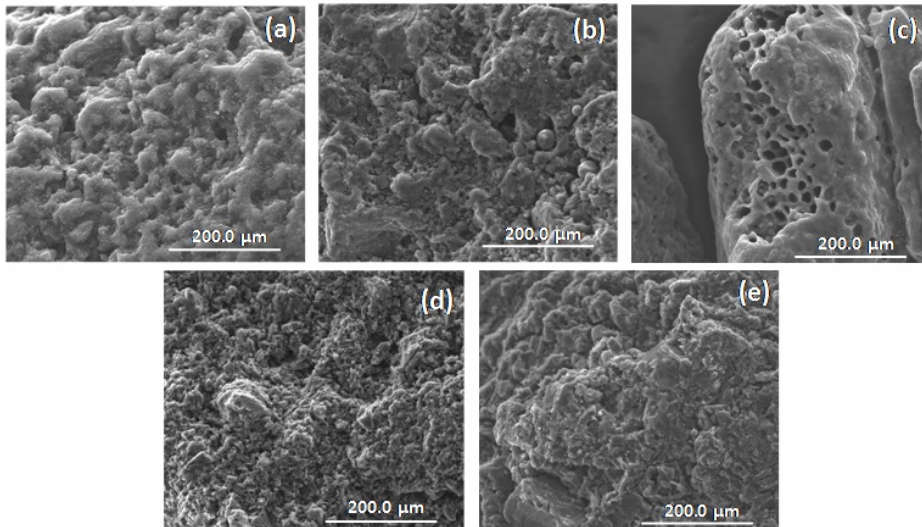
where  $\Delta n$  stands for the standard deviation of the sample, N is number of  $n_{excess}$  values observed and  $n_{FIT}$  is the corresponding mean value calculated by the modified Langmuir equation 7 [44].

### 3. Results and Discussion

#### 3.1. Material properties

Figure 2 presents the morphology of five commercial activated carbons by SEM analysis. They possess two types of morphology: granular (CGRAN, GAC 1240, and ROx 0.8) or pellet (CNR 115 and RX 1.5). In terms of surface roughness, at the scale of  $200 \mu\text{m}$ , CGRAN has a hollow-channel form when all four other materials have a rough porous surface.

**Figure 2:** SEM images of five studied activated carbons: a) CNR-115, b) RX 1.5, c) CGRAN, d) ROX 0.8 and e) GAC 1240 at  $200 \mu\text{m}$  scale.



Along with the SEM images, the  $\text{N}_2$  adsorption/desorption isotherms at 77 K for 5 activated carbons as well as their pore size distributions were published previously in Peredo et al [42]. The  $\text{N}_2$  adsorption/desorption capacities of the five ACs range widely from  $300$  to  $600 \text{ cm}^3 \text{ g}^{-1}$  AC at  $P/P_0 = 1$ . CNR-115 is found to have the highest  $\text{N}_2$  adsorption capacity while GAC 1240 absorbed  $\text{N}_2$  significantly less than the other activated carbons. Indeed, the isotherms on RX 1.5, ROX 0.8, CNR-115, and GAC 1240 give type I behavior, where the presence of a saturation limit indicates the completion of a single monolayer of  $\text{N}_2$  at the material surface [52]. Meanwhile, CGRAN carries type IV isotherm, representing a finite multi-layer formation corresponding to a complete filling of the capillaries, which leads to the deduction of a wide distribution of pore sizes for this AC [53].

In terms of pore size distribution, the particle size of activated carbons also differs widely [42]. While CGRAN and CNR-115 own a broad distribution of pore sizes from  $0.7 \text{ nm}$  to  $1.2 \text{ nm}$  in one peak, RX 1.5, ROX 0.8 have 2 distinct peaks at  $0.7 \text{ nm}$  and  $1.8 \text{ nm}$ . Meanwhile, GAC 1240 possesses a single peak of micropores at  $0.6 \text{ nm}$ , indicating that this activated carbon is more microporous than the others. These findings are consistent with the previous suggestion about CGRAN, that its pores rather have similar sizes.

On the other hand, the influence of porosity and specific surface of absorbent has been proven to affect gas adsorption capacity [54, 55]. In this case, the values of BET areas vary from 982 (GAC 1240) to 1714  $m^2 g^{-1}$  (CNR-115), belong to usual value range of activated carbons [21, 56–59]. Moreover, along with the highest BET areas, CNR-115 and RX 1.5 also own a great proportion of microporous volume (0.64 and 0.61  $cm^3 g^{-1}$  respectively). CGRAN has the most important total pore volume (0.99  $cm^3 g^{-1}$ ) but also the highest mesopore volume (0.54  $cm^3 g^{-1}$ ) due to the high amount of  $H_3PO_4$  during activation, which leads into the average value of BET area [60]. This result approved the two previously published experimental data of nitrogen adsorption/desorption isotherms and pore size distributions, where it was suggested that there was the presence of an important volume of mesopore in CGRAN [42]. Meanwhile, ROX 0.8 possesses a low mesopore volume (0.16  $cm^3 g^{-1}$ ) but also a relatively low micropore volume (48  $cm^3 g^{-1}$ ), therefore carries the similar BET areas value as CGRAN. In the case of GAC 1240, due to the low proportion of  $V_{meso}$  and the low total pore volume (0.56  $cm^3 g^{-1}$ ), this activated carbon is considered least porous having the smallest BET area (982  $m^2 g^{-1}$ ).

### 3.2. Adsorption isotherms

Tables 3 - 5 and Figure 3 present the experimental results of the 5 above-described activated carbons on methane, ethane, and propane at 303K. All isotherms belong to type I which indicates the monolayer isotherms of physisorption as described in Langmuir's theory of adsorption. In other words, the adsorption uptake increased rapidly at low pressure and then saturated upon the pressure augmentation when the pores are gradually filled [61]. All activated carbons showed a major difference between the adsorption capacities, as the adsorbed quantity of ethane and propane was significantly higher than methane.

**Table 3**

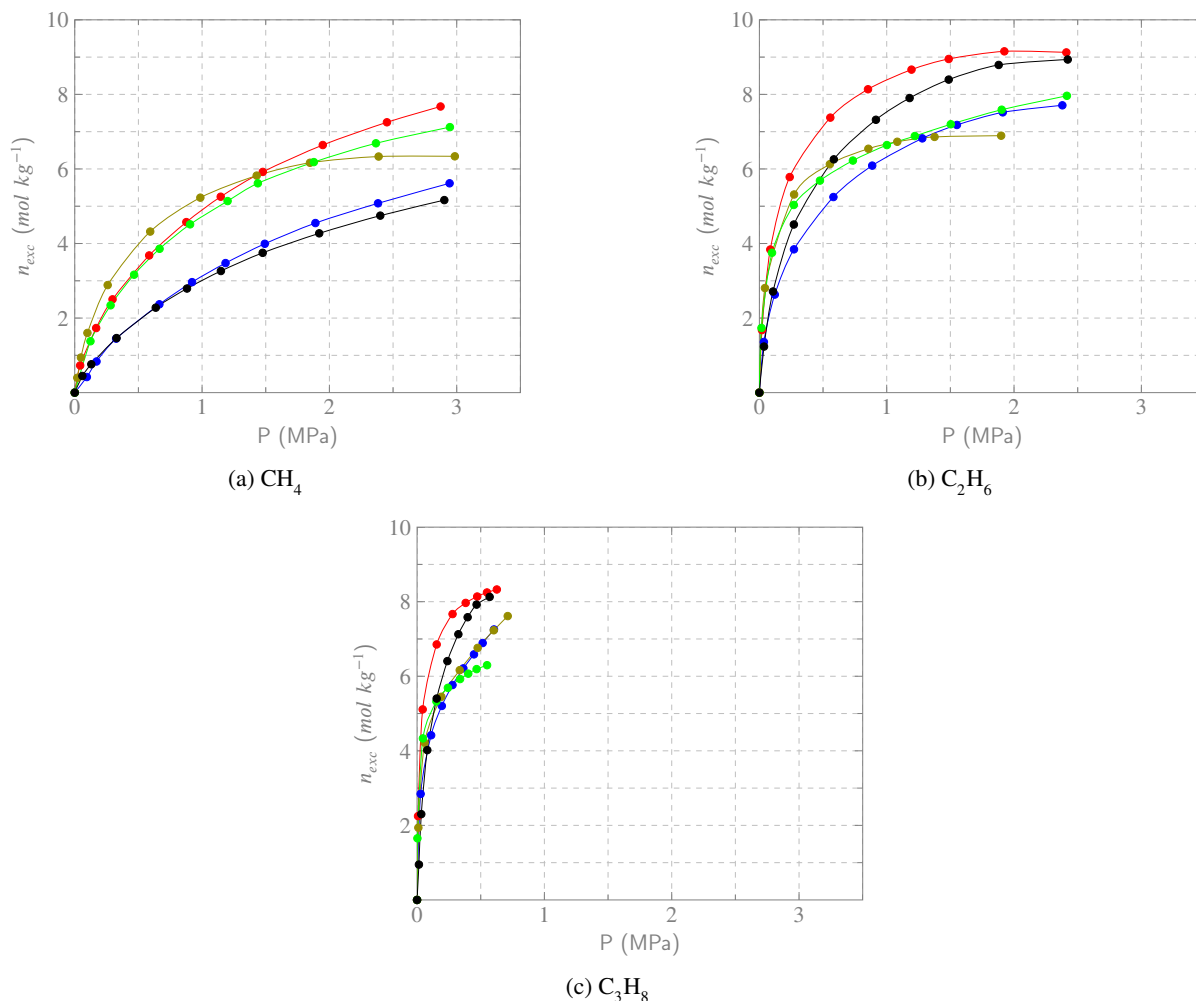
Experimental results of the adsorption of methane on five activated carbons at 303K

RX 1.5		RX 0.8		CGRAN		CNR-115		GAC 1240	
$P_{ads}$ (MPa)	$n_{excess}$ ( $mol kg^{-1}$ )								
0.04	0.73	0.12	1.38	0.10	0.42	0.06	0.45	0.02	0.40
0.17	1.73	0.28	2.34	0.17	0.84	0.13	0.76	0.05	0.94
0.30	2.50	0.47	3.16	0.33	1.45	0.33	1.46	0.10	1.60
0.58	3.68	0.67	3.86	0.66	2.37	0.64	2.28	0.26	2.88
0.88	4.57	0.91	4.51	0.92	2.96	0.88	2.79	0.59	4.32
1.15	5.26	1.20	5.14	1.18	3.47	1.15	3.26	0.99	5.23
1.48	5.92	1.44	5.61	1.49	3.99	1.48	3.75	1.43	5.82
1.95	6.64	1.88	6.18	1.89	4.55	1.92	4.27	1.85	6.17
2.45	7.25	2.37	6.69	2.38	5.08	2.40	4.75	2.39	6.33
2.87	7.68	2.95	7.12	2.94	5.61	2.90	5.16	2.99	6.34

Indeed, in the case of RX 1.5, the adsorption capacity for ethane achieved 9.12  $mol kg^{-1}$  at 2.41 MPa while there was only 7.25 mol of methane adsorbed per kilogram of this activated carbon. In addition, at a low working pressure (0.50 MPa), the propane adsorption capacity already leveled up to 8.09  $mol kg^{-1}$  while the ones for methane and ethane are 3.68 and 7.37  $mol kg^{-1}$  respectively. Likewise, at 1.9 MPa, CNR-115 underwent an adsorption capacity of 8.79  $mol kg^{-1}$  for ethane in relation to 4.17  $mol kg^{-1}$  for methane whilst the same capacity for propane attained at 0.57 MPa. ROx 0.8 had a less important adsorption capacity when 1 kilogram adsorbed only 5.14 mole of methane or 6.44 mol of ethane at 1.2 MPa. The same results also happened to CGRAN, having 5.08 and 7.71  $mol kg^{-1}$  as methane and ethane adsorption capacities and reached 7.26  $mol kg^{-1}$  as propane capacities at 0.604 MPa. In the same way, at 1.0 MPa the measured  $CH_4$  adsorption capacity of GAC 1240 was 5.23  $mol kg^{-1}$  while for ethane and propane, it adsorbed 6.7 and 7.6  $mol kg^{-1}$  respectively.

This phenomenon can be attributed that at low and intermediate pressures, the interaction between propane and the surface of the adsorbent is much higher than methane. Being linear molecules, the more carbon atoms in the chain, the stronger the covalent bond created between alkane molecules and the surface of the activated carbon. For that reason, at low pressure, propane gets adsorbed the most, thus ethane adsorbs the second and methane adsorbed the least [62].

**Figure 3:** Adsorption isotherms of natural gas components at 303 K on five activated carbons: RX 1.5 (red), ROx 0.8 (green), CNR-115 (black), CGRAN (blue) and GAC 1240 (olive).



$\Delta n = 1\%$ ,  $\Delta P = 0.01$  MPa,  $\Delta T = 0.1$  K

This explanation is also consistent with the argument of Pino-Perez et al., that porous materials adsorb preferentially long-chain molecules than short-chain molecules in a study on propane, pentane, and heptane adsorption by using Ecosorb activated carbon [63]. In addition, the strong interactions of ethane and propane with the adsorbents can also be described by Van der Waals's attractive force based on the polarizability of the gas molecules. Indeed, since the polarizability of propane ( $62.9 \times 10^{25} \text{ cm}^3$ ) is greater than ethane ( $44.3 \times 10^{25} \text{ cm}^3$ ) and methane ( $25.93 \times 10^{25} \text{ cm}^3$ ), propane is expected to be the most attracted onto the surface of adsorbents [2].

Despite the higher uptakes, a plateau was observed for C<sub>2</sub>H<sub>6</sub> and C<sub>3</sub>H<sub>8</sub> isotherms of most activated carbons i.e the maximal filling of micro-pores at 303K. Once entering a higher pressure zone, bigger pores start to be filled by the adsorbate. As propane and ethane have longer carbon chains, their rotation and translation get limited, leading to rapid saturation compared to methane. The saturation is clearly observed in the case of RX 1.5, ROx 0.8, and GAC 1240, whose volume of mesopores are low. They possess  $0.20$ ,  $0.16$  and  $0.20 \text{ cm}^3 \text{ g}^{-1}$  as mesopores volume respectively. This finding is in agreement with the study of Mhaskar et al., where the C<sub>3</sub>H<sub>8</sub> adsorption capacity on silica gel in the range of 0 - 1 bar is significantly higher than ethane and methane ones [64].

In general, RX 1.5, ROx 0.8 and GAC 1240 adsorbed methane molecules more than CNR-115 and CGRAN. Indeed, the surface acidity of CNR-115 and CGRAN are reported to be higher than other commercial activated carbons due to the initial chemical activation [65]. As methane is an inert compound, together with the pore blockage of the

**Table 4**

Experimental results of the adsorption of ethane on five activated carbons at 303K.

RX 1.5		RX 0.8		CGRAN		CNR-115		GAC 1240	
$P_{ads}$ (MPa)	$n_{excess}$ (mol kg <sup>-1</sup> )								
0.02	1.68	0.02	1.74	0.04	1.36	0.04	1.24	0.04	2.81
0.09	3.84	0.10	3.75	0.12	2.63	0.11	2.71	0.27	5.31
0.24	5.78	0.27	5.03	0.27	3.84	0.27	4.51	0.55	6.13
0.56	7.38	0.48	5.69	0.58	5.25	0.58	6.26	0.86	6.54
0.85	8.14	0.73	6.23	0.89	6.09	0.92	7.32	1.08	6.73
1.49	8.95	1.22	6.88	1.55	7.18	1.49	8.40	1.90	6.89
1.92	9.15	1.50	7.20	1.91	7.52	1.88	8.79		
2.41	9.13	1.90	7.59	2.38	7.71	2.42	8.94		
		2.42	7.96						

**Table 5**

Experimental results of the adsorption of propane on five activated carbons at 303K.

RX 1.5		RX 0.8		CGRAN		CNR-115		GAC 1240	
$P_{ads}$ (MPa)	$n_{excess}$ (mol kg <sup>-1</sup> )								
0.01	2.25	0.00	1.65	0.03	2.84	0.01	0.95	0.01	1.94
0.04	5.11	0.05	4.33	0.11	4.42	0.03	2.30	0.06	4.22
0.15	6.85	0.15	5.32	0.19	5.20	0.08	4.02	0.19	5.45
0.28	7.67	0.24	5.69	0.28	5.76	0.15	5.40	0.34	6.16
0.38	7.97	0.34	5.92	0.36	6.21	0.24	6.41	0.48	6.76
0.47	8.14	0.40	6.07	0.45	6.59	0.32	7.13	0.60	7.23
0.55	8.25	0.47	6.19	0.52	6.89	0.40	7.58	0.71	7.61
0.63	8.33	0.55	6.30	0.60	7.26	0.47	7.92		
						0.57	8.13		

functional groups, the acidic surface tends to adsorb less than basic ones. This outcome is consistent with the findings of Contreras et al. that the presence of acidic functionalities disfavors the CH<sub>4</sub> uptakes and the basic surface is thought to be responsible for the improvement on CH<sub>4</sub> adsorption [66]. In reference to the CO<sub>2</sub> adsorption capacity, it also seems to be coherent to Peredo et al. [42]. As the surface of RX 1.5 and ROx 0.8 are more basic, they adsorbed more CO<sub>2</sub> pure gas than CNR-115 and CGRAN.

On the other hand, it was observed that not only the C<sub>2</sub>H<sub>6</sub> and C<sub>3</sub>H<sub>8</sub> isotherms, but also the CH<sub>4</sub> isotherm of GAC 1240 saturated considerably faster than other ACs due to its minimal micro-pores and mesopores volumes. Indeed, since GAC 1240 owns only 0.36 and 0.20 cm<sup>3</sup> g<sup>-1</sup> micro-pores and mesopores respectively, at low working pressure, most of its pores filled quickly, leading to fewer spaces for gas molecules at high pressure. The same scenario happened to C<sub>2</sub>H<sub>6</sub> isotherm on RX 1.5 and ROx 0.8, the ethane uptake saturated at 2 MPa, justifying the inferior mesopores volume (0.20 cm<sup>3</sup> g<sup>-1</sup> and 0.16 cm<sup>3</sup> g<sup>-1</sup> respectively).

In the case of C<sub>3</sub>H<sub>8</sub> isotherms, it is necessary to note that the interval of working pressure is reduced due to the limit of gas-liquid transition of propane. However, it was noticed that the results for C<sub>3</sub>H<sub>8</sub> are in coherence with CH<sub>4</sub> and C<sub>2</sub>H<sub>6</sub>, especially in the case of low mesoporous activated carbons like RX 1.5 and ROx 0.8. Here, RX 1.5 showed the highest propane uptakes and saturated at 0.7 MPa. The saturation was also witnessed clearly in ROx 0.8 at 0.5 MPa.

### 3.3. Langmuir fitting parameters

Langmuir fitting parameters of three adsorbates for five adsorbents are presented in Table 6. These parameters are considered accurate as the deviations  $\Delta n$  are relatively low. Furthermore, the relationship between the BET surface of each activated carbon and its maximum Langmuir adsorption capacity is also presented in Figure 4a. This linear regression proved an adequate correlation for methane (blue squares,  $R^2 = 0.902$ ), ethane (red diamonds,  $R^2 = 0.968$ ) and propane (yellow diamonds,  $R^2 = 0.980$ ). In all cases, the larger the BET surface is, the more important the maximum Langmuir becomes. The relation between  $n_L$  and the pore volumes of each activated carbons including micropores, mesopores, and total pores are also established in Figure 4b - 4d. The dependence of  $n_L$  on  $V_{\text{micro}}$  also show and analogous trend i.e the adsorption capacities increase along with the increment of  $V_{\text{micro}}$ . However, there is no clear linear relation is noticed like the BET surface area. This outcome is consistent with the precedent findings of Peredo et al. and Ortiz, the higher BET surface area is responsible for the higher maximum adsorption capacity since it is related directly to the number of available physisorption sites [42, 67].

Sample	Compound	$p_L$ (MPa)	$n_L$ ( $mol\ kg^{-1}$ )	$\Delta n$
RX 1.5	CH <sub>4</sub>	1.09	10.79	0.008
	C <sub>2</sub> H <sub>6</sub>	0.18	10.29	0.016
	C <sub>3</sub> H <sub>8</sub>	0.03	8.82	0.015
CNR-115	CH <sub>4</sub>	1.79	8.45	0.003
	C <sub>2</sub> H <sub>6</sub>	0.38	10.98	0.015
	C <sub>3</sub> H <sub>8</sub>	0.13	9.03	0.010
ROx 0.8	CH <sub>4</sub>	0.94	9.62	0.006
	C <sub>2</sub> H <sub>6</sub>	0.20	11.62	0.024
	C <sub>3</sub> H <sub>8</sub>	0.08	9.20	0.026
CGRAN	CH <sub>4</sub>	2.24	10.28	0.002
	C <sub>2</sub> H <sub>6</sub>	0.38	9.31	0.016
	C <sub>3</sub> H <sub>8</sub>	0.09	8.02	0.018
GAC 1240	CH <sub>4</sub>	0.40	7.44	0.008
	C <sub>2</sub> H <sub>6</sub>	0.07	7.24	0.009
	C <sub>3</sub> H <sub>8</sub>	0.05	7.75	0.021

**Table 6**

Langmuir fitting parameters of adsorption isotherms of methane, ethane, propane on five commercial activated carbons at 303K.

## Adsorption of natural gas components on activated carbons

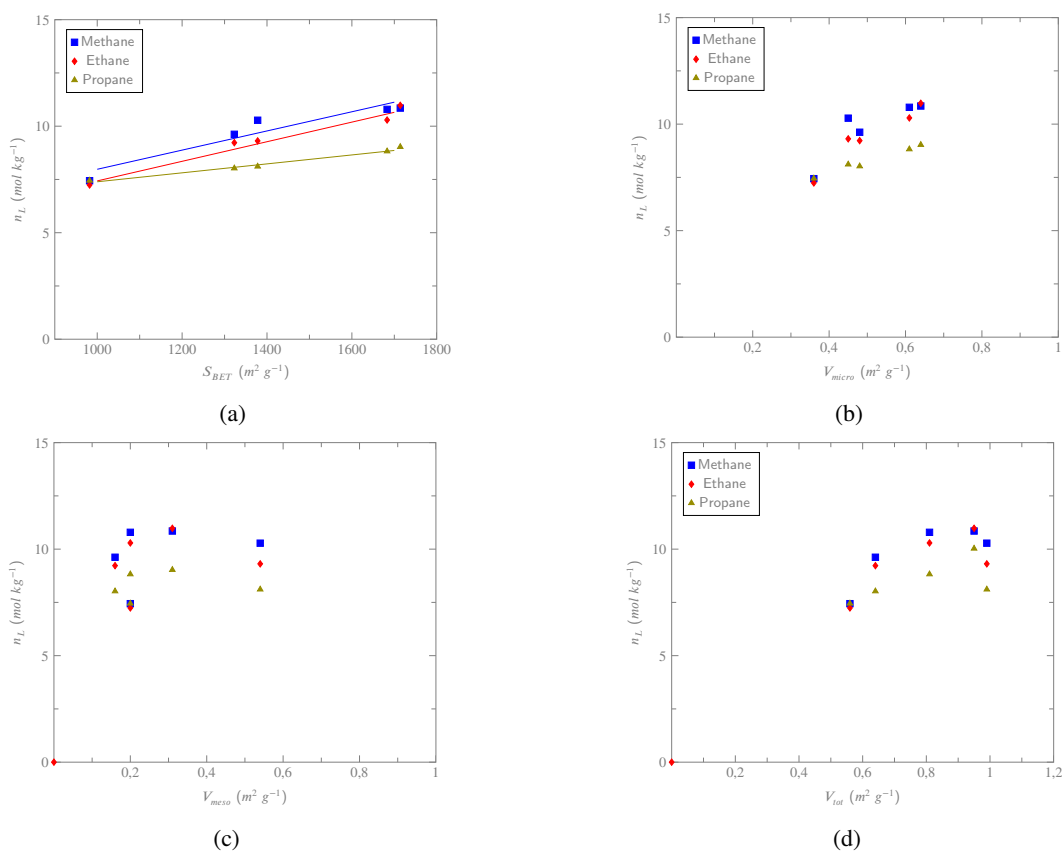


**Figure 4:** Maximum Langmuir capacity at 303K as a function of the (a) BET surface areas, (b) micro-pores volumes, (c) meso-pores volume and (d) total pores volume.

### 3.4. Comparison with other activated carbons in literature

#### 3.4.1. Methane adsorption

Methane adsorption onto activated carbons is commonly published in the literature because this compound exists in both natural gas and raw biogas as a main component. The comparison of methane uptakes of several similar activated carbons (reported in Vargas et al., Tabatabaei Shirazani et al., and Peredo-Macilla et al.) are presented in Table 7 [35, 68, 69].

**Table 7**

Methane uptakes of RX 1.5 and CNR-115 in comparison with other adsorbents in literature.

Sample	Reference	Working conditions	CH <sub>4</sub> adsorption capacity ( <i>mol kg<sup>-1</sup></i> )
RX 1.5	This work	303K and 1 MPa	5.1
CNR-115	This work	303K and 1 MPa	3.1
AC-H <sub>3</sub> PO <sub>4</sub>	[35]	298K and 1 MPa	3.0
MP48	[68]	298 K and 1 MPa	2.4
MCa2	[68]	298 K and 1 MPa	4.6
HS-KOH1:2	[69]	298K and 1 MPa	5.2

As observed, the methane uptakes of activated carbons range widely depending on the textural properties and surface chemistry of the adsorbent. For example, AC-H<sub>3</sub>PO<sub>4</sub> is an olive stones-based activated carbon activated by H<sub>3</sub>PO<sub>4</sub> that had inferior specific surface area (1178 m<sup>2</sup> g<sup>-1</sup>) but superior methane adsorption performance. This

outcome can be attributed to the original surface chemistry of the precursor and the activation process. In the same way, MP48 was also activated by  $H_3PO_4$  that had a lower BET surface ( $1368 \text{ m}^2 \text{ g}^{-1}$ ) and micropore volume ( $0.37 \text{ cm}^3 \text{ g}^{-1}$ ) but the methane uptake of MP48 at 1 MPa was only  $2.4 \text{ mol kg}^{-1}$  compared to  $3.1 \text{ mol kg}^{-1}$  of CNR-115. On the other hand, the morphology of MCa2 was close to CNR-115 ( $S_{\text{BET}} = 1700 \text{ m}^2 \text{ g}^{-1}$ ,  $V_{\text{micro}} = 0.64 \text{ cm}^3 \text{ g}^{-1}$ ) but this activated carbon was activated by  $CaCl_2$ , which may improve the affinity of its surface with  $CH_4$  molecules and enhanced the adsorption capacity [68]. In the case of HS-KOH1:2, the KOH treatment is proved to increase the  $CH_4$  adsorption by widening pores and adjusting the affinity with the adsorbate. However, the  $CH_4$  isotherm of HS-KOH1:2 was quickly saturated, indicating that this adsorbent did not possess enough mesopores to adsorb methane at high pressure [69].

### 3.4.2. Ethane adsorption

Liang et al. [70, 71], Wang et al. [72] and Pires et al. [73] carried out previously ethane adsorption isotherms on different activated carbons from various precursors and activation agents. The experimental outcomes are shown on in Table 8.

**Table 8**

Ethane uptakes of RX 1.5 and CNR-115 in comparison with other adsorbents in literature.

Sample	Reference	Working conditions	$C_2H_6$ adsorption capacity ( $\text{mol kg}^{-1}$ )
RX 1.5	This work	303K and 1.2 MPa	8.7
CNR-115	This work	303K and 1.2 MPa	7.9
C-700-3	[70]	298K and 1 MPa	7.2
C-800-3	[70]	298K and 1 MPa	7.1
C-PDA-3	[72]	298K and 1 MPa	6.6
Ni(bdc)(ted) <sub>0.5</sub>	[71]	298K and 1 MPa	5.0
IRMOF-8	[73]	298K and 1 MPa	4.0

At 1 MPa, RX 1.5 and CNR-115 own superior ethane adsorption capacity over C-700-3 and C-800-3 despite the lower BET surfaces. It is because C-700-3 and C-800-3 are rather mesoporous material due to the excess use of KOH as activation agent, which resulted in the low ethane uptakes at low pressure but allows to adsorb ethane at high pressure without being saturated. Similarly, since C-PDA-3 was activated with an increase in KOH/C ratio, some micropores were transformed into mesopores, hence the ethane uptakes is reduced at 1 MPa but it still has room for adsorption at high working pressure. On the other hand, as observed, RX 1.5 and CNR-115 are more microporous hence adsorbed ethane more quickly but also had a faster saturation tendency.

In general, activated carbons have shown their promising adsorption capacity over MOFs. Liang et al. and Pires et al. [71, 73] reported the ethane adsorption capacities of two MOFs Ni(bdc)(ted)<sub>0.5</sub> and IRMOF-8 were 5.0 and  $4.0 \text{ mol kg}^{-1}$  respectively. Meanwhile, the specific surface area and total pore volume of Ni(bdc)(ted)<sub>0.5</sub> were  $1701 \text{ m}^2 \text{ g}^{-1}$  and  $0.79 \text{ cm}^3 \text{ g}^{-1}$ , which were relatively similar to the morphology of RX 1.5 and CNR-115 [71]. Therefore, the inferior performance of MOFs is not only due to the lower BET area but also the weak affinity of adsorbate with the MOF surface. The adsorption capacity is hence thought to be resulted from various factors such as morphology, surface chemistry of the adsorbent and physico-chemical properties of the adsorbate.

### 3.4.3. Propane adsorption

Regarding the propane adsorption, RX 1.5 and CNR-115 also show advantageous capacities in comparison with the MOFs Cu-MOF-74 and Co-MOF-74 by Abedini et al. and the activated carbon Ecosorb by Pino et al. [34, 74]. However, a quick saturation of  $C_3H_8$  adsorption isotherms was observed for all adsorbents, indicating the total micropore filling at low temperature and low pressure due to the high affinity between the long-chain molecules and the force field of the adsorbent.

As with the ethane uptakes, the propane adsorption capacity depends predominantly on the morphology of the adsorbent. Since the BET area and average pore size of the activated carbon Ecosorb were  $1290 \text{ m}^2 \text{ g}^{-1}$  and 0.46 nm, this adsorbent was more microporous than CNR-115 and RX 1.5 and did not own too much available sites for adsorption at high pressure. Consequently, at 0.5 MPa, the propane uptakes of Ecosorb was  $5.7 \text{ mol kg}^{-1}$  while RX

1.5 and CNR-115 reached 8.0-8.1  $\text{mol kg}^{-1}$ . Similarly, in addition to the inferior BET area and micropore volume, Cu-MOF-74 and Co-MOF-74 also had weaker affinity with propane, leading into lower propane uptakes compared to activated carbons.

**Table 9**

Propane uptakes of RX 1.5 and CNR-115 in comparison with other adsorbents in literature.

Sample	Reference	Working conditions	$\text{C}_3\text{H}_8$ adsorption capacity ( $\text{mol kg}^{-1}$ )
RX 1.5	This work	303K and 0.5 MPa	8.1
CNR-115	This work	303K and 0.5 MPa	8.0
Ecosorb	[74]	303K and 0.5 MPa	5.7
Cu-MOF-74	[34]	303K and 0.5 MPa	5.6
Co-MOF-74	[34]	303K and 0.5 MPa	5.4

## 4. Conclusion

The adsorption isotherms of natural gas components which are methane, ethane, and propane were successfully carried out for a series of five commercial activated carbons. Most activated carbons presented the type I isotherm, indicating the highly porous adsorbent with monolayer adsorption. Regarding the three adsorbates, the increase in chain length leads to the preferential adsorption of gaseous molecules as reported in literature [34, 74]. Therefore, all activated carbons showed a greater adsorption capacity on propane than ethane and methane at low pressure. However, once the experimental pressure enters the higher zone i.e micropores are filled, the adsorption of gas molecules on mesoporous adsorbents tends to saturate slower.

Among the studied activated carbons, for ethane and propane adsorption, RX 1.5 and CNR-115 showed superior adsorption capacities of the three gases because they possess not only high BET surface but also adequate volumes of micro-pores and mesopore. Hence, they have a good balance of different porosity to satisfy the low and high-pressure adsorption. This relationship was not noticed previously in the studies of smaller molecules because they can rotate and translate more freely compared to carbon chains.

The obtained data for pure gas adsorption isotherms were well fitted to the Langmuir two parameters model, indicating they are all microporous adsorbent and the surface coverage can be considered monolayer. In terms of the highest maximum Langmuir capacity, RX1.5, CNR-115, and ROx 0.8 showed the highest adsorption capacity of  $\text{CH}_4$ ,  $\text{C}_2\text{H}_6$ , and  $\text{C}_3\text{H}_8$  respectively compared to CGRAN and GAC 1240. The Langmuir adsorption capacity also was found to be influenced directly by the BET area of the adsorbent.

## Declaration of interest

The authors declare that they have no known competing financial interests or personal relationships that could have appeared to influence the work reported in this paper.

## References

- [1] A. Abdullah, I. Idris, I. K. Shamsudin, M. R. Othman, Methane enrichment from high carbon dioxide content natural gas by pressure swing adsorption, *Journal of Natural Gas Science and Engineering* 69 (2019) 102929. doi:10.1016/j.jngse.2019.102929.
- [2] J.-R. Li, R. J. Kuppler, H.-C. Zhou, Selective gas adsorption and separation in metal-organic frameworks, *Chemical Society Reviews* 38 (5) (2009) 1477–1504, publisher: The Royal Society of Chemistry. doi:10.1039/B802426J.
- [3] S. Faramawy, T. Zaki, A. A. E. Sakr, Natural gas origin, composition, and processing: A review, *Journal of Natural Gas Science and Engineering* 34 (2016) 34–54. doi:10.1016/j.jngse.2016.06.030.
- [4] L. Wang, H. Gardeler, J. Gmehling, Model and experimental data research of natural gas storage for vehicular usage, *Separation and Purification Technology* 12 (1) (1997) 35–41. doi:10.1016/S1383-5866(97)00013-0.
- [5] S. Koonaphaddeert, J. Moran, P. Aggarangsi, A. Bunkham, Low pressure biomethane gas adsorption by activated carbon, *Energy for Sustainable Development* 43 (2018) 196–202. doi:10.1016/j.esd.2018.01.010.
- [6] R. Kadam, N. L. Panwar, Recent advancement in biogas enrichment and its applications, *Renewable and Sustainable Energy Reviews* 73 (2017) 892–903. doi:10.1016/j.rser.2017.01.167.

- [7] V. Vrbová, K. Čiáhoťný, Upgrading Biogas to Biomethane Using Membrane Separation, *Energy & Fuels* 31 (9) (2017) 9393–9401, publisher: American Chemical Society. doi:10.1021/acs.energyfuels.7b00120.
- [8] S. Sahota, G. Shah, P. Ghosh, R. Kapoor, S. Sengupta, P. Singh, V. Vijay, A. Sahay, V. K. Vijay, I. S. Thakur, Review of trends in biogas upgradation technologies and future perspectives, *Bioresource Technology Reports* 1 (2018) 79–88. doi:10.1016/j.biteb.2018.01.002.
- [9] D. G. Pahinkar, S. Garimella, A novel temperature swing adsorption process for natural gas purification: Part I, model development, *Separation and Purification Technology* 203 (2018) 124–142. doi:10.1016/j.seppur.2018.04.020.
- [10] I. Angelidaki, L. Treu, P. Tsapekos, G. Luo, S. Campanaro, H. Wenzel, P. G. Kougias, Biogas upgrading and utilization: Current status and perspectives, *Biotechnology Advances* 36 (2) (2018) 452–466. doi:10.1016/j.biotechadv.2018.01.011.
- [11] R. Murad, D. L. Mohamed, M. S. M. Nasir, L. C. Law, I. Idris, M. R. Othman, Flared Gas Emission Control from an Oil Production Platform., *Journal of Physical Science* 30 (2019).
- [12] M. Pardakhti, E. Moharrerri, D. Wanik, S. L. Suib, R. Srivastava, Machine Learning Using Combined Structural and Chemical Descriptors for Prediction of Methane Adsorption Performance of Metal Organic Frameworks (MOFs), *ACS Combinatorial Science* 19 (10) (2017) 640–645, publisher: American Chemical Society. doi:10.1021/acscombsci.7b00056.
- [13] C. M. Simon, J. Kim, D. A. Gomez-Gualdrón, J. S. Camp, Y. G. Chung, R. L. Martin, R. Mercado, M. W. Deem, D. Gunter, M. Haranczyk, D. S. Sholl, R. Q. Snurr, B. Smit, The materials genome in action: identifying the performance limits for methane storage, *Energy & Environmental Science* 8 (4) (2015) 1190–1199, publisher: The Royal Society of Chemistry. doi:10.1039/C4EE03515A.
- [14] G. Lei, Q. Li, H. Liu, Y. Zhang, Selective adsorption of CO<sub>2</sub> by Hex-star phosphorene from natural gas: Combining molecular simulation and real adsorbed solution theory, *Chemical Engineering Science* 231 (2021) 116283. doi:10.1016/j.ces.2020.116283.
- [15] R. Weh, G. Xiao, M. A. Islam, E. F. May, Nitrogen rejection from natural gas by dual reflux-pressure swing adsorption using activated carbon and ionic liquid zeolite, *Separation and Purification Technology* 235 (2020) 116215. doi:10.1016/j.seppur.2019.116215.
- [16] A. Arefi Pour, S. Sharifnia, R. Neishabouri Salehi, M. Ghodrati, Adsorption separation of CO<sub>2</sub>/CH<sub>4</sub> on the synthesized NaA zeolite shaped with montmorillonite clay in natural gas purification process, *Journal of Natural Gas Science and Engineering* 36 (2016) 630–643. doi:10.1016/j.jngse.2016.11.006.
- [17] L. Zhu, X. Lv, S. Tong, T. Zhang, Y. Song, Y. Wang, Z. Hao, C. Huang, D. Xia, Modification of zeolite by metal and adsorption desulfurization of organic sulfide in natural gas, *Journal of Natural Gas Science and Engineering* 69 (2019) 102941. doi:10.1016/j.jngse.2019.102941.
- [18] H. Sui, J. Liu, L. He, X. Li, A. Jani, Adsorption and desorption of binary mixture of acetone and ethyl acetate on silica gel, *Chemical Engineering Science* 197 (2019) 185–194. doi:10.1016/j.ces.2018.12.010.
- [19] Z. Bao, S. Alnemrat, L. Yu, I. Vasiliev, Q. Ren, X. Lu, S. Deng, Kinetic separation of carbon dioxide and methane on a copper metal–organic framework, *Journal of Colloid and Interface Science* 357 (2) (2011) 504–509. doi:10.1016/j.jcis.2011.01.103.
- [20] I. A. A. C. Esteves, M. S. S. Lopes, P. M. C. Nunes, J. P. B. Mota, Adsorption of natural gas and biogas components on activated carbon, *Separation and Purification Technology* 62 (2) (2008) 281–296. doi:10.1016/j.seppur.2008.01.027.
- [21] O. Oginni, K. Singh, G. Oporto, B. Dawson-Andoh, L. McDonald, E. Sabolsky, Effect of one-step and two-step H<sub>3</sub>PO<sub>4</sub> activation on activated carbon characteristics, *Bioresource Technology Reports* 8 (2019) 100307. doi:10.1016/j.biteb.2019.100307.
- [22] S. H. Tang, M. A. Ahmad Zaini, Development of activated carbon pellets using a facile low-cost binder for effective malachite green dye removal, *Journal of Cleaner Production* 253 (2020) 119970. doi:10.1016/j.jclepro.2020.119970.
- [23] L. S. Queiroz, L. K. C. de Souza, K. T. C. Thomaz, E. T. Leite Lima, G. N. da Rocha Filho, L. A. S. do Nascimento, L. H. de Oliveira Pires, K. d. C. F. Faial, C. E. F. da Costa, Activated carbon obtained from amazonian biomass tailings (acai seed): Modification, characterization, and use for removal of metal ions from water, *Journal of Environmental Management* 270 (2020) 110868. doi:10.1016/j.jenvman.2020.110868.
- [24] T. Matsui, S. Imamura, Removal of siloxane from digestion gas of sewage sludge, *Bioresource Technology* 101 (1 SUPPL.) (2010) S29–S32. doi:10.1016/j.biortech.2009.05.037.
- [25] A. Petersson, 14 - Biogas cleaning, in: A. Wellinger, J. Murphy, D. Baxter (Eds.), *The Biogas Handbook*, Woodhead Publishing Series in Energy, Woodhead Publishing, 2013, pp. 329–341. doi:10.1533/9780857097415.3.329.
- [26] E. Menya, P. W. Olupot, H. Storz, M. Lubwama, Y. Kiros, Production and performance of activated carbon from rice husks for removal of natural organic matter from water: A review, *Chemical Engineering Research and Design* 129 (2018) 271–296. doi:10.1016/j.cherd.2017.11.008.
- [27] S. Ahmed, A. Ahmed, M. Rafat, Investigation on activated carbon derived from biomass *Butnea monosperma* and its application as a high performance supercapacitor electrode, *Journal of Energy Storage* 26 (2019) 100988. doi:10.1016/j.est.2019.100988.
- [28] M. L. Pinto, J. Pires, J. Rocha, Porous Materials Prepared from Clays for the Upgrade of Landfill Gas, *The Journal of Physical Chemistry C* 112 (37) (2008) 14394–14402. doi:10.1021/jp803015d.
- [29] H. Rezvani, S. Fatemi, J. Tamnanloo, Activated carbon surface modification by catalytic chemical vapor deposition of natural gas for enhancing adsorption of greenhouse gases, *Journal of Environmental Chemical Engineering* 7 (3) (2019) 103085. doi:10.1016/j.jece.2019.103085.
- [30] S. Chen, M. Tian, Z. Tao, Y. Fu, Y. Wang, Y. Liu, B. Xiao, Effect of swing on removing CO<sub>2</sub> from offshore natural gas by adsorption, *Chemical Engineering Journal* (2019) 122932doi:10.1016/j.cej.2019.122932.
- [31] L. Jiang, A. Gonzalez-Diaz, J. Ling-Chin, A. P. Roskilly, A. J. Smallbone, Post-combustion CO<sub>2</sub> capture from a natural gas combined cycle power plant using activated carbon adsorption, *Applied Energy* 245 (2019) 1–15. doi:10.1016/j.apenergy.2019.04.006.
- [32] G. Carchini, I. Hussein, M. J. Al-Marri, R. Shawabkeh, M. Mahmoud, S. Aparicio, A theoretical study of gas adsorption on calcite for CO<sub>2</sub> enhanced natural gas recovery, *Applied Surface Science* (2019) 144575doi:10.1016/j.apsusc.2019.144575.
- [33] J. Speight, Liquid fuels from natural gas, *Handbook of Alternative Fuel Technologies* (2015) 157–178.
- [34] H. Abedini, A. Shariati, M. R. Khosravi-Nikou, Adsorption of propane and propylene on M-MOF-74 (M=Cu, Co): Equilibrium and kinetic study, *Chemical Engineering Research and Design* 153 (2020) 96–106. doi:10.1016/j.cherd.2019.10.014.
- [35] D. Peredo-Mancilla, I. Ghouma, C. Hort, C. M. Ghimbeu, M. Jeguirim, D. Bessieres, CO<sub>2</sub> and CH<sub>4</sub> Adsorption Behavior of Biomass-Based Activated Carbons, *Energies* 11 (11) (2018) 3136, number: 11 Publisher: Multidisciplinary Digital Publishing Institute. doi:10.3390/

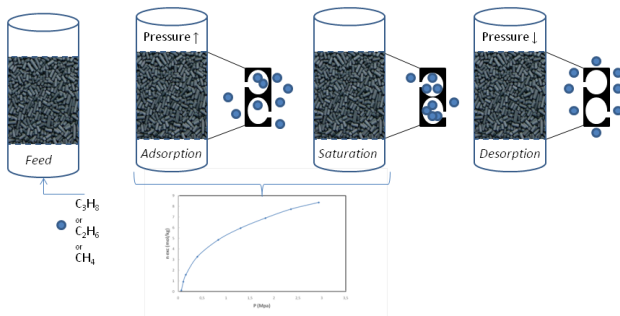
- en11113136.
- [36] C. Corporation, *Reactivation Services* (2016).
- [37] K. Koehlert, *Activated Carbon: Fundamentals and New Applications* (Jul. 2017).
- [38] M. G. Plaza, S. García, F. Rubiera, J. J. Pis, C. Pevida, Post-combustion CO<sub>2</sub> capture with a commercial activated carbon: Comparison of different regeneration strategies, *Chemical Engineering Journal* 163 (1) (2010) 41–47. doi:10.1016/j.cej.2010.07.030.
- [39] B. Aumeier, H. Q. A. Dang, M. Wessling, Preliminary Study on the Application of Temperature Swing Adsorption in Aqueous Phase for Pesticide Removal, *IOP Conference Series: Earth and Environmental Science* 159 (2018) 012013, publisher: IOP Publishing. doi:10.1088/1755-1315/159/1/012013.
- [40] N. O. of Data and Informatics, NIST Chemistry WebBook. doi:https://doi.org/10.18434/T4D303.
- [41] M. Gasparik, A. Ghanizadeh, P. Bertier, Y. Gensterblum, S. Bouw, B. M. Krooss, High-Pressure Methane Sorption Isotherms of Black Shales from The Netherlands, *Energy & Fuels* 26 (8) (2012) 4995–5004. doi:10.1021/ef300405g.
- [42] D. Peredo-Mancilla, C. Hort, M. Jeguirim, C. M. Ghimbeu, L. Limousy, D. Bessieres, Experimental Determination of the CH<sub>4</sub> and CO<sub>2</sub> Pure Gas Adsorption Isotherms on Different Activated Carbons, *Journal of Chemical & Engineering Data* 63 (8) (2018) 3027–3034. doi:10.1021/acs.jced.8b00297.
- [43] A. F. Ismail, K. Khulbe, T. Matsuura, *Gas Separation Membranes: Polymeric and Inorganic*, Springer International Publishing, 2015. doi:10.1007/978-3-319-01095-3.
- [44] R. Ettarh, Common descriptive and analytical statistics in investigative studies, *Radiography* 10 (4) (2004) 299–302. doi:10.1016/j.radi.2004.05.010.
- [45] S. Matteucci, Y. Yampolskii, B. Freeman, I. Pinnau, Transport of Gases and Vapors in Glassy and Rubbery Polymers, in: *Materials Science of Membranes for Gas and Vapor Separation*, Vol. 1, 2006, pp. 1–47, journal Abbreviation: *Materials Science of Membranes for Gas and Vapor Separation*. doi:10.1002/047002903X.ch1.
- [46] H. Swenson, N. P. Stadie, *Langmuir's Theory of Adsorption: A Centennial Review*, Langmuir Publisher: American Chemical Society (Mar. 2019). doi:10.1021/acs.langmuir.9b00154.
- [47] A. M. Awad, S. M. R. Shaikh, R. Jalab, M. H. Gulied, M. S. Nasser, A. Benamor, S. Adham, Adsorption of organic pollutants by natural and modified clays: A comprehensive review, *Separation and Purification Technology* 228 (2019) 115719. doi:10.1016/j.seppur.2019.115719.
- [48] J. Li, Y. Ma, K. Huang, S. Lu, J. Yin, Y. Zhang, Comprehensive polynomial simulation and prediction for Langmuir volume and Langmuir pressure of shale gas adsorption using multiple factors, *Marine and Petroleum Geology* 88 (2017) 1004–1012. doi:10.1016/j.marpetgeo.2017.09.034.
- [49] O. P. Ortiz Cancino, D. Pino Pérez, M. Pozo, D. Bessieres, Adsorption of pure CO<sub>2</sub> and a CO<sub>2</sub>/CH<sub>4</sub> mixture on a black shale sample: Manometry and microcalorimetry measurements, *Journal of Petroleum Science and Engineering* 159 (2017) 307–313. doi:10.1016/j.petrol.2017.09.038.
- [50] PubChem, Ethane - structure, chemical names, physical and chemical properties, classification, patents, literature, biological activities, safety/hazards/toxicity information, supplier lists, and more.
- [51] I. for Occupational Safety and Health of the German Social Accident Assurance, Propane.
- [52] S. Lowell, J. E. Shields, Adsorption isotherms, in: S. Lowell, J. E. Shields (Eds.), *Powder Surface Area and Porosity*, Springer Netherlands, Dordrecht, 1984, pp. 11–13. doi:10.1007/978-94-009-5562-2\_3.
- [53] M. Sultan, T. Miyazaki, S. Koyama, Optimization of adsorption isotherm types for desiccant air-conditioning applications, *Renewable Energy* 121 (2018) 441–450. doi:10.1016/j.renene.2018.01.045.
- [54] M. Belhachemi, M. Jeguirim, L. Limousy, F. Addoun, Comparison of NO<sub>2</sub> removal using date pits activated carbon and modified commercialized activated carbon via different preparation methods: Effect of porosity and surface chemistry, *Chemical Engineering Journal* 253 (2014) 121–129. doi:10.1016/j.cej.2014.05.004.
- [55] Y. J. Cao, W. Q. Shen, J. F. Shao, N. Burlion, Influences of micro-pores and meso-pores on elastic and plastic properties of porous materials, *European Journal of Mechanics - A/Solids* 72 (2018) 407–423. doi:10.1016/j.euromechsol.2018.06.003.
- [56] C. Saka, BET, TG–DTG, FT-IR, SEM, iodine number analysis and preparation of activated carbon from acorn shell by chemical activation with ZnCl<sub>2</sub>, *Journal of Analytical and Applied Pyrolysis* 95 (2012) 21–24. doi:10.1016/j.jaap.2011.12.020.
- [57] A. R. Hidayu, N. F. Mohamad, S. Matali, A. S. A. K. Sharifah, Characterization of Activated Carbon Prepared from Oil Palm Empty Fruit Bunch Using BET and FT-IR Techniques, *Procedia Engineering* 68 (2013) 379–384. doi:10.1016/j.proeng.2013.12.195.
- [58] S. M. Kharrazi, N. Mirghaffari, M. M. Dastgerdi, M. Soleimani, A novel post-modification of powdered activated carbon prepared from lignocellulosic waste through thermal tension treatment to enhance the porosity and heavy metals adsorption, *Powder Technology* 366 (2020) 358–368. doi:10.1016/j.powtec.2020.01.065.
- [59] S. Wang, H. Nam, H. Nam, Preparation of activated carbon from peanut shell with KOH activation and its application for H<sub>2</sub>S adsorption in confined space, *Journal of Environmental Chemical Engineering* 8 (2) (2020) 103683. doi:10.1016/j.jece.2020.103683.
- [60] P. González-García, Activated carbon from lignocellulosics precursors: A review of the synthesis methods, characterization techniques and applications, *Renewable and Sustainable Energy Reviews* 82 (2018) 1393–1414. doi:10.1016/j.rser.2017.04.117.
- [61] K. C. Ng, M. Burhan, M. W. Shahzad, A. B. Ismail, A Universal Isotherm Model to Capture Adsorption Uptake and Energy Distribution of Porous Heterogeneous Surface, *Scientific Reports* 7 (1) (2017) 10634, number: 1 Publisher: Nature Publishing Group. doi:10.1038/s41598-017-11156-6.
- [62] Y. K. Ponraj, B. Borah, Separation of methane from ethane and propane by selective adsorption and diffusion in MOF Cu-BTC: A molecular simulation study, *Journal of Molecular Graphics and Modelling* 97 (2020) 107574. doi:10.1016/j.jmkgm.2020.107574.
- [63] D. Pino Pérez, *Étude Expérimentale de l'Adsorption de gaz sur des solides micro ou meso-poreux à haute pression. Application a des problématiques du génie pétrolier.*, Ph.D. thesis, Université de Pau et des Pays de l'Adour (2013).
- [64] P. R. Mhaskar, A. S. Moharir, *Natural Gas Treatment Using Adsorptive Separation, Natural Gas - Extraction to End Use* Publisher: IntechOpen

- (Oct. 2012). doi:10.5772/53269.
- [65] D. Peredo-Mancilla, C. Matei Ghimbeu, B.-N. Ho, M. Jeguirim, C. Hort, D. Bessieres, Comparative study of the CH<sub>4</sub>/CO<sub>2</sub> adsorption selectivity of activated carbons for biogas upgrading, *Journal of Environmental Chemical Engineering* 7 (5) (2019) 103368. doi:10.1016/j.jece.2019.103368.
- [66] M. Contreras, G. Lagos, N. Escalona, G. Soto-Garrido, L. R. Radovic, R. Garcia, On the methane adsorption capacity of activated carbons: in search of a correlation with adsorbent properties, *Journal of Chemical Technology & Biotechnology* 84 (11) (2009) 1736–1741, eprint: <https://onlinelibrary.wiley.com/doi/pdf/10.1002/jctb.2239>. doi:10.1002/jctb.2239.
- [67] O. Ortiz Cancino, Etude expérimentale de l'adsorption du méthane dans des gaz de schistes colombiens et de la séparation méthane/dioxyde de carbone, PhD Thesis, Pau (2018).
- [68] D. P. Vargas, L. Giraldo, J. C. Moreno-Piraján, Carbon dioxide and methane adsorption at high pressure on activated carbon materials, *Adsorption* 19 (6) (2013) 1075–1082. doi:10.1007/s10450-013-9532-5.
- [69] M. Tabatabaei Shirazani, H. Bakhshi, A. Rashidi, M. Taghizadeh, Starch-based activated carbon micro-spheres for adsorption of methane with superior performance in ANG technology, *Journal of Environmental Chemical Engineering* 8 (4) (2020) 103910. doi:10.1016/j.jece.2020.103910.
- [70] W. Liang, Y. Zhang, X. Wang, Y. Wu, X. Zhou, J. Xiao, Y. Li, H. Wang, Z. Li, Asphalt-derived high surface area activated porous carbons for the effective adsorption separation of ethane and ethylene, *Chemical Engineering Science* 162 (2017) 192–202. doi:10.1016/j.ces.2017.01.003.
- [71] W. Liang, F. Xu, X. Zhou, J. Xiao, Q. Xia, Y. Li, Z. Li, Ethane selective adsorbent Ni(bdc)(ted)0.5 with high uptake and its significance in adsorption separation of ethane and ethylene, *Chemical Engineering Science* 148 (2016) 275–281. doi:10.1016/j.ces.2016.04.016.
- [72] X. Wang, Y. Wu, X. Zhou, J. Xiao, Q. Xia, H. Wang, Z. Li, Novel C-PDA adsorbents with high uptake and preferential adsorption of ethane over ethylene, *Chemical Engineering Science* 155 (2016) 338–347. doi:10.1016/j.ces.2016.08.026.
- [73] J. Pires, M. L. Pinto, V. K. Saini, Ethane Selective IRMOF-8 and Its Significance in Ethane–Ethylene Separation by Adsorption, *ACS Applied Materials & Interfaces* 6 (15) (2014) 12093–12099, publisher: American Chemical Society. doi:10.1021/am502686g.
- [74] D. Pino, F. Plantier, D. Bessières, Adsorption of Alkanes in the Dense Vapor Phase on a Microporous Activated Carbon, *Journal of Chemical & Engineering Data* 62 (5) (2017) 1716–1724, publisher: American Chemical Society. doi:10.1021/acs.jced.7b00175.

## Graphical Abstract

### Determination of methane, ethane and propane on activated carbons by experimental pressure swing adsorption method

Bich Ngoc Ho, David Pino Perez, Deneb Peredo Mancilla, Joseph Diaz, Cécile Hort, David Bessieres, Camélia Matei Ghimbeu



## Highlights

### **Determination of methane, ethane and propane on activated carbons by experimental pressure swing adsorption method**

Bich Ngoc Ho, David Pino Perez, Deneb Peredo Mancilla, Joseph Diaz, Cécile Hort, David Bessieres, Camélia Matei Ghimbeu

- The adsorption capacity of gas molecules was proved to depend on the material properties of each activated carbon.
- Specific surface areas play a major role in the scale of adsorption capacity.
- The influence of the carbon chain on the saturation of adsorption isotherms was verified.
- Adsorption isotherms of studied gases on commercial activated carbons were well fit by the modified Langmuir model.